COBEM 2023 27TH INTERNATIONAL CONGRESS OF MECHANICAL ENGENEERING

ABCM Brazilian Society of Mechanical Sciences and Engineering
27th ABCM International Congress of Mechanical Engineering
December 04-08, 2023, Florianópolis-SC, Brazil

COB-2023-1636
LAMINAR SEPARATION BUBBLES ANALYSIS OF GIESEKUS FLUID FLOW

Beatriz Liara Carreira
Universidade de São Paulo, Instituto de Ciências Matemáticas e de Computação, São Carlos, SP
liara.carreira@usp.br

Daniel Rodríguez
ETSIAE-UPM (School of Aeronautics), Universidad Politécnica de Madrid, Spain
daniel.rodriguez@upm.es

Elmer Mateus Gennaro
UNESP, Campus de São João da Boa Vista, SP
elmer.gennaro@unesp.br

Analice Costacurta Brandi
UNESP, Faculdade de Ciências e Tecnologia, Presidente Prudente, SP
analice.brandi@unesp.br

Leandro Franco de Souza
Universidade de São Paulo, Instituto de Ciências Matemáticas e de Computação, São Carlos, SP
lefraso@icmc.usp.br

Abstract. *Laminar separation bubbles arise due to the combined effect of airfoil curvature and angle of attack when an adverse pressure gradient appears after peak suction. If this pressure gradient is strong enough, the laminar boundary layer is separated. This creates the recirculation zone, where the fluid moves more slowly and in the opposite direction. This region is unstable, so the laminar flow will eventually transition to a turbulent regime. Therefore, a complete understanding of the transition phenomenon is essential. The hydrodynamic stability analysis is carried out to predict these changes. There are studies in this direction considering Newtonian fluids, but this is still an open question in the case of non-Newtonian fluids. Thus, this work aims to investigate the base flow that simulates a two-dimensional laminar separation bubble in an incompressible flow considering a non-Newtonian fluid using the Giesekus model, analyzing how some characteristics behave when non-Newtonian parameters are varied. In the future, the global linear stability theory will be used to investigate these separation bubbles non-Newtonian, using a bi-global technique.*

Keywords: *separation bubble, Giesekus fluid, bi-global stability analysis, laminar-turbulent transition*

1. INTRODUCTION

The process of changes that affects the laminar flow, leading it to the turbulent regime, is known as laminar-turbulent transition. The hydrodynamic stability analysis is carried out to predict these changes. The transition from laminar to turbulent flow is generally associated with base flow instabilities. When this transition occurs in separation bubbles, one-, two-, and three-dimensional structures can be generated. The transition details depend entirely on the type of external disturbances imposed on the amount of separation.

Flow separation in wall-bounded flows occurs frequently in nature and in technological applications. For example, the flow separation causes an abrupt loss of lift on an airfoil when the angle of attack reaches the critical or stall value (Hammond and Redekopp, 1998). The laminar separation bubble is a type of separate flow of considerable practical interest.

Laminar separation bubbles arise due to the combined effect of airfoil curvature and angle of attack when an adverse pressure gradient appears after peak suction. If this pressure gradient is strong enough, the laminar boundary layer is separated. The structure of a separate region includes a recirculation region, where the fluid moves more slowly and in the opposite direction to the oncoming flow. Hydrodynamic instability dominates the dynamics of the separated layer, strongly amplifying external disturbances and leading to laminar–turbulent transition even at very low free-stream turbulence levels (Rodríguez *et al.*, 2021).

In this sense, hydrodynamic stability analysis can be used to investigate the transition phenomenon in separation

flows. Unlike the classic theory of local linear stability, a global linear stability analysis solves the equations of the base flow with more than one non-homogeneous spatial direction. The introduction of a modal formulation for the linear disturbances converts the system of linearized equations into an eigenvalue problem with respect to the base flow. As in the classical theory of local linear stability, the eigenvalue determines whether the corresponding eigenvector grows in time or space and provides information about the frequency of the linear disturbance, while the eigenvector describes the spatial structure of the linear disturbance (Taira *et al.*, 2017). The solution to the eigenvalue problem is global modes. They describe disturbances that develop over base flows that vary non-homogeneously in two (bi-global) or three (tri-global) spatial directions.

Recent studies have used global linear stability analysis to investigate the presence of convective and absolute instability mechanisms and explain the origin of instability and transition to turbulence without external disturbances in laminar separation bubbles (Rodríguez *et al.*, 2013, 2021). Applications of global stability analysis have been widely studied, mainly in Newtonian fluid flows. In this sense, one of the focuses of interest in this work is to use global linear stability analysis to predict complex phenomena that may result from the behavior of non-Newtonian fluids, for example.

Non-Newtonian fluids are characterized by a non-linear relationship between shear stress and strain rate. In particular, some of these fluids have viscous and elastic properties simultaneously and are called viscoelastic fluids. Dealing with viscoelastic fluid flows is a challenge, mainly because, in addition to the possibilities of conservation of mass and momentum, a constitutive equation related to the strain tensor is needed (Carreira, 2020).

In this sense, this work aims to investigate the base flow, which simulates a laminar separation bubble of a non-Newtonian fluid. This base flow has been generated using a Direct Numerical Simulation code. In this sense, the non-Newtonian separation bubbles are obtained from the variation of the polymeric viscosity coefficient and characterized in terms of their length and peak reverse flow, making it possible to compare them with the Newtonian flow. Results of stability analysis of the non-Newtonian laminar separation bubble using the bi-global code will be included in future work.

2. MATHEMATICAL FORMULATION

The flow is assumed to be unsteady, non-Newtonian, bi-dimensional and incompressible. The conservation of mass (continuity) and conservation of momentum equations governing the flow in the dimensionless form is given by

$$\nabla \cdot \mathbf{u} = 0, \tag{1}$$

$$\frac{\partial \mathbf{u}}{\partial t} + \nabla \cdot (\mathbf{uu}) = -\nabla p + \frac{\beta_n}{Re}\nabla^2 \mathbf{u} + \nabla \cdot \mathbf{T}, \tag{2}$$

where $\mathbf{u} = [u, v]^T$ denotes the velocity field in the directions x and y, respectively, t is the time, p is the pressure and $\mathbf{T}$ is the non-Newtonian extra-stress tensor (symmetric), given by $\mathbf{T} = \begin{bmatrix} T^{xx} & T^{xy} \\ T^{xy} & T^{yy} \end{bmatrix}$.

The dimensionless parameter $Re = U_\infty L/\nu$ is associated with the Reynolds number, where L and U_∞ denote length and velocity scales, respectively, and ν is the kinematic viscosity of the fluid. The dimensionless solvent viscosity coefficient $\beta_n = \eta_s/\eta_0$ controll the amount of Newtonian solvent, where $\eta_0 = \eta_s + \eta_p$ denotes the total shear viscosity, being η_s and η_p the Newtonian solvent and polymeric viscosities, respectively.

In this paper, we worked with viscoelastic fluid flow governed by the non-linear Giesekus constitutive equation (Giesekus, 1982), which is given by

$$\mathbf{T} + Wi\overset{\triangledown}{\mathbf{T}} + \alpha_G \frac{WiRe}{1-\beta_n}(\mathbf{T}\cdot\mathbf{T}) = \frac{1-\beta_n}{Re}(\nabla\mathbf{u} + \nabla\mathbf{u}^\top), \tag{3}$$

where α_G is the mobility parameter that regulates the shear thinning behavior of the fluid ($0 \leq \alpha_G \leq 1$), $\mathbf{T}\cdot\mathbf{T}$ is a tensor product and $\overset{\triangledown}{\mathbf{T}}$ is the upper-convected derivative. The Weissenberg number is denoted by the dimensionless parameter $Wi = \lambda U_\infty/L$, where λ is the relaxation time of the fluid.

3. BASE FLOW: MODEL LAMINAR SEPARATION BUBBLES

An inverse formulation of similar incompressible boundary-layer equations is used to obtain the base flow for a stationary two-dimensional laminar separation bubble. The streamwise and wall-normal coordinates are denoted by x and y, and their respective velocity components by u and v. Furthermore, we denote the boundary-layer edge velocity U_∞ and the kinematic viscosity ν. When considering a base flow subject to pressure gradient variations, the potential flow is assumed to be approximated by the function $U_\infty = x^m$.

Therefore, the dimensionless coordinate of the boundary layer η can be written as

$$\eta = y\sqrt{\frac{m+1}{2}\frac{U_\infty}{\nu\, x}} = y\sqrt{\frac{m+1}{2}\frac{1}{\nu}}\, x^{\frac{m-1}{2}}, \tag{4}$$

where m is a parameter that quantifies the free-stream pressure gradient. Employing this parameter, imposing an adverse pressure gradient on the boundary layer flow is possible and thus obtaining a separation flow.

Defining the streamfunction Ψ, such that

$$u = \frac{\partial \Psi}{\partial y} \quad \text{and} \quad v = -\frac{\partial \Psi}{\partial x}, \tag{5}$$

then an equation for the transformed streamfunction $f(\eta)$ is obtained,

$$f(\eta) = \Psi / \sqrt{\frac{2}{m+1}\nu\, x^{\frac{m+1}{2}}}. \tag{6}$$

After the substitution of these variables in the streamwise momentum equation, the following equation for $f(\eta)$ is obtained

$$f''' + \frac{m+1}{2} f f'' + m(1 - f'^2) = 0, \tag{7}$$

which is the Falkner-Skan equation (Schilichting, 1979). This problem is solved subject to the boundary conditions

$$f(0) = 0; \quad f'(0) = 0 \quad \text{and} \quad f(\eta \to \infty) = 1. \tag{8}$$

When solving the Eq. (7), the streamwise and wall-normal dimensional velocity components are obtained using the transformation

$$u = \frac{\partial \Psi}{\partial y} = f'(\eta) x^m = U_\infty f'(\eta), \tag{9}$$

$$v = -\frac{\partial \Psi}{\partial x} = -\sqrt{\frac{m+1}{2}\nu x^{m-1}} \left(f(\eta) + \frac{m-1}{m+1}\eta f'(\eta) \right). \tag{10}$$

3.1 Direct Numerical Simulation

The structure of a separation bubble is described in Fig. 1. Due to the curvature of the airfoil and the angle of attack, there is an adverse pressure gradient after the suction peak. If this pressure gradient is strong enough, the boundary layer will separate and give rise to a separate mixed layer. The laminar separation bubble appears after the boundary layer separation point.

In this work, the bubble was reproduced using a typical configuration for this type of problem, considering a flat plate boundary layer with an adverse pressure gradient at the top of the computational domain. Non-slip and impermeability conditions apply to the plate.

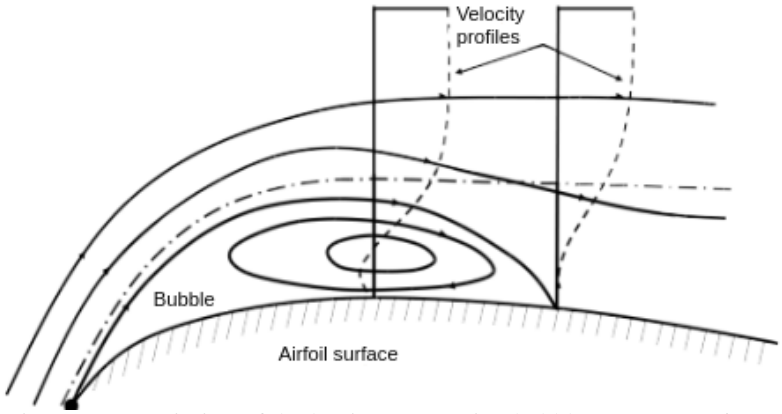

Figure 1: Description of the laminar separation bubble (Horton, 1968).

In sense, a direct numerical simulation for a non-Newtonian boundary layer flow subject to an adverse pressure gradient is performed using the solution of the Falkner-Skan equation (Schilichting, 1979) as initial conditions. This procedure allows us to obtain the velocity and non-Newtonian tensor components $\overline{\mathbf{q}} = (U, V, T^{xx}, T^{xy}, T^{yy})$ for a laminar separation bubble.

In the direct numerical simulation, to simplify the problem and eliminate the pressure treatment in the momentum equations, we chose the vorticity-velocity formulation (Brandi *et al.*, 2017). Then, the two-dimensional vorticity ω_z is defined by

$$\omega_z = \frac{\partial U}{\partial y} - \frac{\partial V}{\partial x}. \tag{11}$$

Applying such formulation, the direct numerical simulation code resolves the system composed by Eqs. (12) – (17),

$$\frac{\partial U}{\partial x} + \frac{\partial V}{\partial y} = 0, \tag{12}$$

$$\frac{\partial^2 V}{\partial x^2} + \frac{\partial^2 V}{\partial y^2} = -\frac{\partial \omega_z}{\partial x}, \tag{13}$$

$$\frac{\partial \omega_z}{\partial t} + \frac{\partial \omega_z}{\partial x}U + \frac{\partial \omega_z}{\partial y}V = \frac{\beta}{Re}\left[\frac{\partial^2 \omega_z}{\partial x^2} + \frac{\partial^2 \omega_z}{\partial y^2}\right] - \frac{\partial^2 T^{xy}}{\partial x^2} - \frac{\partial^2 T^{yy}}{\partial x \partial y} + \frac{\partial^2 T^{xx}}{\partial y \partial x} + \frac{\partial^2 T^{xy}}{\partial y^2}, \tag{14}$$

$$T^{xx} + Wi\left(\frac{\partial T^{xx}}{\partial t} + U\frac{\partial T^{xx}}{\partial x} + V\frac{\partial T^{xx}}{\partial y} - 2T^{xx}\frac{\partial U}{\partial x} - 2T^{xy}\frac{\partial U}{\partial y}\right) + \alpha_G \frac{WiRe}{1-\beta}\left(T^{xx^2} + T^{xy^2}\right) = = 2\frac{1-\beta}{Re}\frac{\partial U}{\partial x}, \tag{15}$$

$$T^{xy} + Wi\left(\frac{\partial T^{xy}}{\partial t} + U\frac{\partial T^{xy}}{\partial x} + V\frac{\partial T^{xy}}{\partial y} - T^{xx}\frac{\partial V}{\partial x} - T^{yy}\frac{\partial U}{\partial y}\right) + \alpha_G \frac{WiRe}{1-\beta}\left(T^{xy}\left(T^{xx} + T^{yy}\right)\right) = = \frac{1-\beta}{Re}\left(\frac{\partial V}{\partial x} + \frac{\partial U}{\partial y}\right), \tag{16}$$

$$T^{yy} + Wi\left(\frac{\partial T^{yy}}{\partial t} + U\frac{\partial T^{yy}}{\partial x} + V\frac{\partial T^{yy}}{\partial y} - 2T^{xy}\frac{\partial V}{\partial x} - 2T^{yy}\frac{\partial V}{\partial y}\right) + \alpha_G \frac{WiRe}{1-\beta}\left(T^{xy^2} + T^{yy^2}\right) = = 2\frac{1-\beta}{Re}\frac{\partial V}{\partial y}, \tag{17}$$

where Eq. (12) is the continuity equation, Eq. (13) is the Poisson equation for the V velocity component, obtained deriving Eq. (11) with respect to x. Equation (14) is obtained by deriving the momentum equation in direction y with respect to x and subtracting the derivative of the momentum equation in direction x with respect to y. Finally, Eqs. (15) – (17) are the Giesekus model equations for the non-Newtonian tensor in two-dimensional cartesian coordinates.

The numerical method used for the temporal discretization of the equations that model the flow and the components of the extra-stress tensor of the viscoelastic flow is a classic fourth-order Runge-Kutta integration scheme. In particular, considering that the region of interest in the y direction is close to the rigid boundary, we seek to reduce the computational cost and, at the same time, obtain a better numerical resolution in this region through a mesh stretching strategy in the direction normal to the wall. Spatial derivatives are solved using high-order compact finite difference schemes, which require the solution of tridiagonal linear systems. The FAS (Full Approximation Storage) scheme solves the Poisson equation using a Line Successive Overrelaxation (LSOR) method.

4. NUMERICAL RESULTS

The following results refer to the base flow generated in a Direct Numerical Simulation. The simulation considered $U_\infty = 0.532$ m/s, $L = 0.0254$ m and $\nu = 1.5 \times 10^{-5}$ m^2/s, resulting in a Reynolds number $Re = 900.85$.

For base flow, the domain of numerical integration extends from $x_0 = 0.6$ to $x_{max} = 33.2$ in the streamwise direction and from $y_0 = 0$ to $y_{max} = 3.5$ in the normal direction. In this case, x represents the extension of the plate surface,

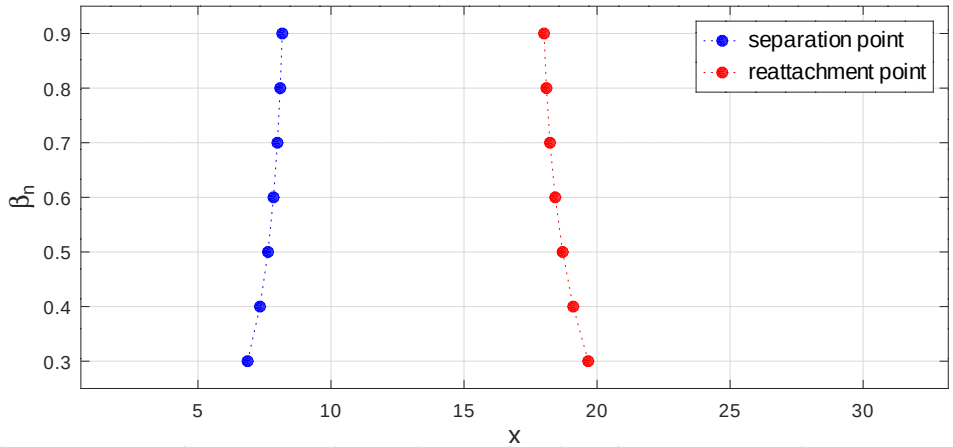

Figure 2: Extent of the reversed flow region as a function of the non-Newtonian parameter β_n.

while y denotes the height of the flow. The following parameters were adopted for the numerical simulation: the number of points in the streamwise and normal directions are $imax = 1305$ and $jmax = 193$, respectively, being the distance between two consecutive points in the direction x, $\Delta x = 0.025$. Discretization in the y direction was performed using a mesh with a stretch factor of 10%.

The parameter α_G of the Giesekus model was fixed at 0.5 while the coefficient β_n varied between 0.3 and 0.9 with increments of 0.1 for a Weissenberg number fixed at $Wi = 1.0$. For these configurations, Fig. 2 presents the length of the

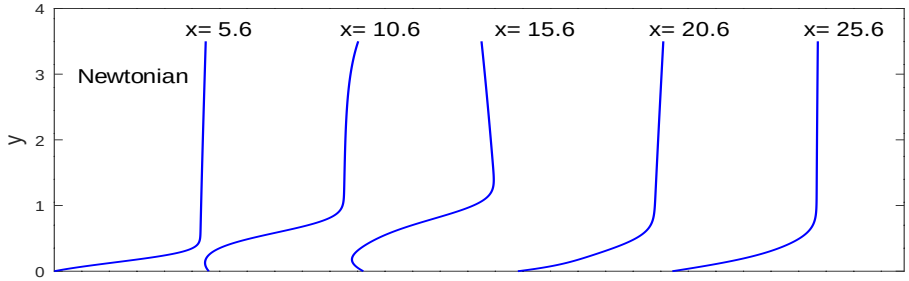

(a)

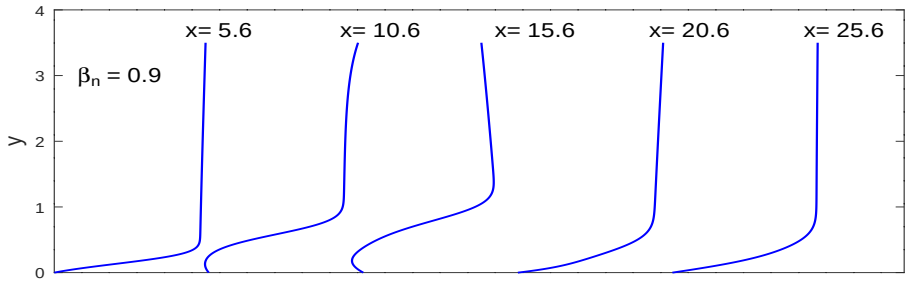

(b)

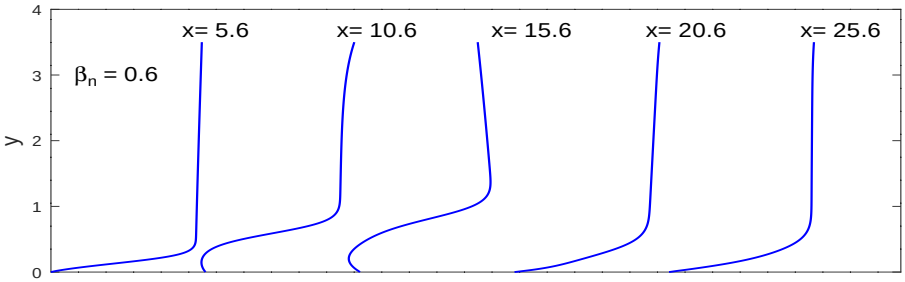

(c)

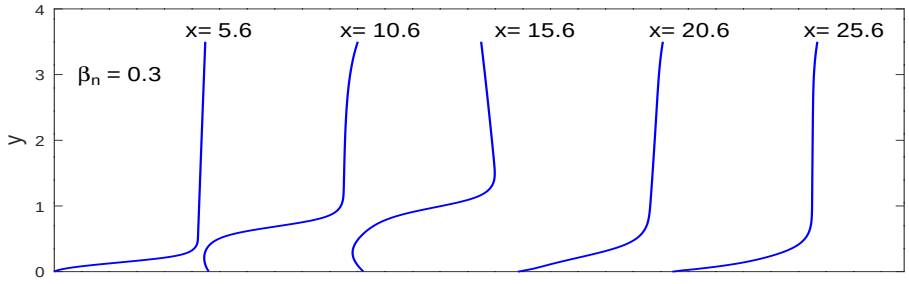

(d)

Figure 3: Evolution of streamwise velocity profiles U: (a) Newtonian case and non-Newtonian cases: (b) $\beta_n = 0.9$; (c) $\beta_n = 0.6$ and (d) $\beta_n = 0.3$.

laminar separation bubble obtained as a function of the variation of β_n. As mentioned, β_n is the coefficient that controls the amount of Newtonian solvent in the fluid. That is, there is a more significant non-Newtonian contribution in the fluid as the value of β_n decreases. Consequently, as β_n approaches one, the fluid configuration approaches the Newtonian configuration. Figure 2 demonstrates that for the highest values of β_n, the boundary layer separation and reattachment points approach the results obtained for the Newtonian case, whose flow separation occurs at $x = 8.17$ and reattachment at $x = 18.01$. In addition, as we increase the non-Newtonian contribution of the fluid, the length of the separation bubble increases, with the separation point moving to the left and the reattachment point moving to the right.

Through Fig. 3, it is possible to observe the evolution of the velocity profile U in the streamwise direction. In Figs. 3(b)-3(d) are represented the velocity profiles in some fixed positions in the x direction considering non-Newtonian flows, and they can be compared with the Newtonian flow in Fig. 3(a). It is possible to see that from $x = 10.6$, there is already the presence of reverse flow followed by the development of the boundary layer after the reattachment.

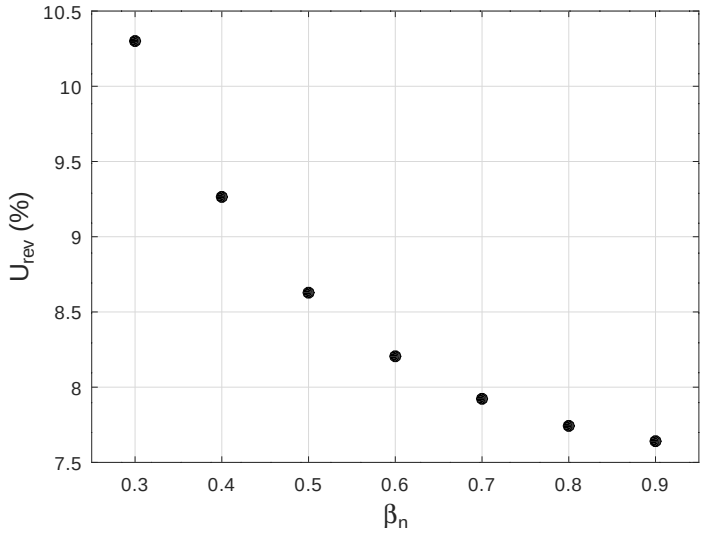

Figure 4: Reverse flow level obtained in non-Newtonian laminar separation bubbles.

An essential piece of information closely related to the development and evolution of hydrodynamic instability in separation flows is the recirculation level of the flow, which is a percentage quantity measured by the ratio between the maximum reverse velocity and the free stream velocity flow. From Fig. 4, it can be seen that there is an increase in the reverse flow level as the value of β_n decreases. On the other hand, as β_n increases, the flow recirculation level approaches the observed value for the Newtonian case, which corresponds approximately to $U_{rev} = 7.6\%$.

5. CONCLUSIONS

So far, it has been possible to generate the base flow for a two-dimensional boundary layer separation flow of a viscoelastic and incompressible fluid from a Direct Numerical Simulation code. Based on the information extracted from the results, it was possible to evaluate the behavior of the boundary layer separation flow, observing characteristics such

as the flow separation and reattachment points, separation bubble length and flow recirculation level.

From variations in non-Newtonian parameters, it was possible to see that the separation bubble length is more significant in flows with more outstanding non-Newtonian contributions. Another phenomenon observed is that the increase in the non-Newtonian contribution in the fluid, controlled by the parameter β_n, induces an increase in the level of reverse flow.

6. ACKNOWLEDGEMENTS

The authors acknowledge the National Council for Scientific and Technological Development (CNPq) or the research grant received during the development of this study. The research was carried out using the computational resource of the Center for Mathematical Applied to Industry (CeMEAI), funded by FAPESP (Process Number 2013/07375-0).

7. REFERENCES

Brandi, A.C., Mendonça, M.T. and de Souza, L.F., 2017. "Comparação de DNS e LST para o escoamento de Poiseuille do fluido Oldroyd-B". In *13º Congresso Ibero-americano de Engenharia Mecânica*. Lisboa, Portugal.

Carreira, B.L., 2020. *Aplicação da Transformação Núcleo-Conformação na Estabilidade de Escoamentos de Fluidos Viscoelásticos*. Master's thesis, FCT-UNESP, Presidente Prudente.

Giesekus, H., 1982. "A simple constitutive equation for polymer fluids based on the concept of deformation-dependent tensorial mobility". *Journal of Non-Newtonian Fluid Mechanics*, Vol. 11, pp. 69–109.

Hammond, D.A. and Redekopp, L.G., 1998. "Local and global instability properties of separation bubbles". *Eur. J. Mech.*, Vol. 17, pp. 145–164.

Horton, H., 1968. *Laminar separation in two and three-dimensional incompressible flow*. Ph.D. thesis, University of London.

Rodríguez, D., Gennaro, E.M. and Juniper, M.P., 2013. "The two classes of primary modal instability in laminar separation bubbles". *J. Fluid Mech.*, Vol. 744, p. R4.

Rodríguez, D., Gennaro, E.M. and Souza, L.F., 2021. "Self-excited primary and secondary instability of laminar separation bubbles". *J. Fluid Mech.*, Vol. 906, p. A13.

Schilichting, H., 1979. *Boundary-Layer Theory*. McGraw-Hill, IncH.

Taira, K., Brunton, S.L., Dawson, S.T., Rowley, C.W., Colonius, T., McKeon, B.J. and Ukeiley, L.S., 2017. "Modal analysis of fluid flows: An overview". *AIAA Journal*, Vol. 55, p. 4013–4041.

8. RESPONSIBILITY NOTICE

The authos are solely responsible for the printed material included in this paper.